Pol. J. Environ. Stud. Vol. 29, No. 5 (2020), 3675-3682
DOI: *10.15244/pjoes/117694* ONLINE PUBLICATION DATE: 2020-04-29

Original Research

A Novel 3D-QSA^{2}R Model Assisted with a Log-Normalized Method and Its Application in Molecular Modification

Minghao Li, Wenhui Zhang, Yilin Hou, Ruihao Sun, Yu Li*

The Moe Key Laboratory of Resources and Environmental Systems Optimization,
North China Electric Power University, Beijing, China

Received: 10 November 2019
Accepted: 30 January 2020

Abstract

The long-range migration ability of persistent organic pollutants was characterized by both K_{OA} and P_L. It is difficult for a traditional model of 3D-QSAR to capture the relationship between the double activities of pollutants and their structures. To this end, a log-normalized method was employed to treat a given data set (K_{OA} and P_L values) to obtain a comprehensive activity (Z) that represents the long-range migration ability of polyhalogenated biphenyls. Then, the relationship between the comprehensive activity of polyhalogenated biphenyls and their structures could be constructed; the proposed model was named the three-dimensional quantitative structure-double-activities relationship (3D-QSA^{2}R) model. Two new PCB-52 molecules with a reduced ability for long-range migration were designed after analyses of the contour maps, with Z values increasing significantly by 30.44-41.30%, and the environmental persistence, bioconcentration and biotoxicity decreased by 3.37-8.99%, 26.86-26.73% and -1.17-3.50%, respectively, compared with those of PCB-52. logK_{OA} and logP_L values of the novel modified PCB-52 were predicted as 3.20-4.57% and 74.57-79.19%, respectively, by the EPI database software, and these values showed a consistent increasing trend with the Z values predicted by 3D-QSA^{2}R, indicating that the established 3D-QSA^{2}R could be used to deal with the relationship between the multi-activities of organic pollutants and their structures.

Keywords: polychlorinated biphenyls, long-range migration, log-normalized, double-activities 3D-QSA^{2}R, molecular modification

Introduction

Although chemical substances are beneficial to human life, large quantities of these chemicals flow into the environment as they are used and released. The transport of chemical substances in multiple environmental media widens the damage scope of these chemicals to the ecological environment and increases the difficulty of controlling chemical pollution. Atmospheric transport is the major pathway for the transport and redistribution of chemical pollutants in the environment of land and water bodies [1-2]. Approximately 70% to 90% of chronic disease risks

*e-mail: liyuxx8@hotmail.com

in humans are probably due to chemical substance pollution in the environment [3]. In 1990, with the promulgation of the "U.S. Pollution Prevention Act of 1990", all countries agreed to employ the highly realistic concept of green chemistry [4]. The concept of green chemistry encourages the use of effective technical means to design environmentally friendly chemicals. The concept of green chemistry to encourage humans to effectively control the sources of chemicals is very different from the practices of traditional industry. Therefore, it has been increasingly important to find an effective design method for environmentally friendly molecules with low migration ability.

Polychlorinated biphenyls (PCBs), as traditional persistent organic pollutants (POPs), have the characteristics of environmental persistence, biological toxicity, bioaccumulation and long-range migration [5-8]. PCB production stopped in most countries by the early 1980s. However, many high-migration PCBs still exist in electrical systems and garbage dumps. These compounds may flow into the surface environment of non-pollution sources by dry or wet deposition processes under long-range migration from the atmosphere [5]. The migration ability of PCB molecules is directly related to their physicochemical properties and the special symmetry of their molecular structure. Molecular modification studies of PCBs in terms of their low migration ability and environmental friendliness still provide a useful reference for the theoretical design of other persistent organic pollutant molecules and new chemical substances.

Liquid vapour pressure (P_L) and octanol-air partition coefficients (K_{OA}) are important parameters to characterize the long-range migration ability of pollutants in the atmosphere. These parameters represent two mechanisms describing the process for gas-particle partitioning of chemical pollutants: adsorption onto the particle surface or absorption into organic matter in aerosols for migration [9]. A single parameter may not be able to fully characterize the mechanism of chemical pollutants in the process of atmospheric system migration [10-11]. A two-dimensional quantitative structure-property relationship (2D-QSPR) model was applied to predict the P_L values of polybrominated diphenyl ether (PBDE), polychlorinated diphenyl ether (PCDE) and various organic molecules, and studied the relationship between molecular structure descriptors and the parameter P_L [12-14]. The 2D-QSPR model was employed to predict the K_{OA} values of various organic molecules and evaluated the accuracy of the prediction model [15]. The hologram quantitative structure-activity relationship (HQSAR) and three-dimensional quantitative structure-activity relationship (3D-QSAR) models established in literature were used to predict the K_{OA} values of PCBs [16-17]. The prediction models constructed in the above literature fail to take into account both action mechanisms at the same time, which makes it impossible to fully characterize the atmospheric migration of pollutants. Therefore, a normalization treatment method to obtain the comprehensive activity value that can take into account both migration activity parameters of P_L and K_{OA} was introduced in this paper. A 3D-QSAR comprehensive model of three activities treated by the fuzzy normalization mathematical method (similar to the method proposed in this manuscript) was successfully established and employed to molecular modification [18]. Common normalization methods include the max-min method [19], Z-score method [20], Tanh-estimators method [21], and log-normalized method [22]. The log-normalized method is extensively used in medicine, business, engineering [23-24] and other fields due to the relatively simple data normalization process, but there are few reports on its application in the construction of a three-dimensional quantitative structure-double-activities relationship (3D-QSA^{2}R) model and molecular design.

In this paper, the parameters of double migration activities normalized by the log-normalized method are determined, and the comprehensive activity values are calculated, which represent low migration activity. The use of comprehensive activity values to construct the 3D-QSA^{2}R model to characterize the relationship between the multi-activities of organic pollutants and their structure is explored. In view of the design and modification requirements of environmentally friendly chemicals, the application of this work could hope to achieve the purpose of simultaneous improvement of multiple environmental activities from source. Besides, this study was applied for controlling pollutants and pollution control of the atmosphere. Combined with the substitution design of PCB molecules for low long-range migration abilities, it is possible to control the risk of chemical pollution from the source, thus providing a reference for the theoretical design of PCB derivatives and of other environmentally friendly chemicals.

Materials and Methods

Constructing the 3D-QSA^{2}R Model Normalized by the Log-Normalized Method

In this paper, the P_L experimental value of other halogenated biphenyls, such as polybrominated biphenyls and polybrominated diphenyl ethers, was employed as a supplement due to the limited P_L experimental values of PCB molecules (Table 1) [25].

The P_L and K_{OA} experimental values of 30 halogenated biphenyls from the literature were normalized by the log-normalized method and were used to generate the comprehensive activity values (Z) of double parameters by a no-weight redistribution process. The Z values are log-normalized as follows:

$$Z = [\frac{\log K_{OA}(x)}{\max(\log K_{OA})} + \frac{-\log P_L(x)}{-\max(\log P_L)}] \times \frac{1}{2}$$

Table 1. Experimental values ($\log K_{OA}$ and $-\log P_L$) of halogenated biphenyls [25].

Molecule	$\log K_{OA}$	$-\log P_L$
PCB-52	8.76	1.73
PCB-101	9.35	2.40
PCB-138	10.04	3.21
PCB-153	9.91	3.05
PCB-180	10.52	3.76
PBB-15	8.50	1.78
PBB-26	9.13	2.36
PBB-31	9.21	2.43
PBB-49	9.83	3.02
PBB-103	10.46	3.60
PBB-153	12.00	5.04
PBDE-1	7.24	0.53
PBDE-10	8.12	1.56
PBDE-13	8.55	1.95
PBDE-15	8.64	2.01
PBDE-30	9.02	2.34
PBDE-32	9.28	2.65
PBDE-35	9.61	2.90
PBDE-37	9.68	2.99
PBDE-47	10.34	3.49
PBDE-66	10.49	3.82
PBDE-75	10.15	3.30
PBDE-77	10.70	3.79
PBDE-99	11.28	4.59
PBDE-116	11.36	4.45
PBDE-119	11.52	4.45
PBDE-153	12.15	5.03
PBDE-155	11.86	4.92
PBDE-166	12.63	5.63
PBDE-181	13.48	6.43

Comparative molecular field analysis (CoMFA), a type of QSAR model, was applied to establish the 3D-QSA²R model using the *Z* values as the dependent variables and using the structure parameters of halogenated biphenyls as the independent variables. The lowest energy conformational optimization was performed for 30 halogenated biphenyls by SYBYL-X 2.0 software. The Gasteiger-Huckel charge was loaded, and the Powell energy gradient method was utilized. The maximum amount of optimization was 10000, and the energy convergence was limited to 0.005 kJ/mol. Optimized molecular structures of 30 halogenated biphenyls were stored in the database, and BDE-181 with the maximum *Z* value was selected as the template molecule to align the other compounds.

The molecular force field of the CoMFA model is classified into the electrostatic field (E) and the steric field (S), and the default threshold value is 30 kcal/mol; the grid was automatically generated, and then using the sp^3 carbon probe atom for the computational grid point distribution size, system default values were selected as the other parameters to generate the molecular force field parameters [26]. The model applied partial least squares (PLS) analysis to determine the linear relationship between the *Z* values of molecules and their fields. In the PLS analysis, the leave-one-out procedure was utilized to cross-verify the training set compounds. The cross-validation coefficient (q^2) and the optimal number of components (n) were calculated to verify the reliability of the CoMFA model. Moreover, the other assessment parameters in the PLS analysis, such as the non-cross-validation coefficient (r^2), the standard error of estimate (SEE) and the Fischer test value (F), as well as the contribution rate of the electrostatic field and the steric field to the molecular migration activity of PCBs, were obtained by the non-validation procedure [17]. The cross-validation method is utilized to obtain the final model parameters such as the correlation coefficient (r^2_{pred}) and the standard error parameters (SEPs) to test the external forecasting ability of the CoMFA model.

Analysis of the Contour Maps for a Lower Migration Ability of the PCB Molecule Based on the CoMFA Model

Z values need to increase because the migration ability of PCB molecules is inversely proportional to these values. The contour maps of the CoMFA model were classified into two types of electrostatic fields (E) and steric fields (S). The contour maps of the steric field were divided into green and yellow regions. The green region indicates where the introduction of substituent groups with larger volumes than the chlorine atom is conducive to increasing the *Z* value, while the yellow region requires the introduction of substituent groups with smaller volumes than the chlorine atom to be conducive to increasing the *Z* value. The contour maps of the electrostatic field were divided into blue and red regions, respectively. The blue region requires the introduction of positive substituent groups compared with the chlorine atom, while the red region requires the introduction of negative substituent groups relative to the chlorine atom to increase the *Z* value [27]. The effects on the site substitution characteristics of PCBs by two types of force fields were summarized and applied to molecular modification. Furthermore, the smaller the Z value of the PCBs, the greater the migration ability. The most representative PCB-52 molecule in the training set, with the lowest Z value and the highest migration ability,

was selected as the target molecule for the study of molecular modification.

Assessment of the Functional Parameters and POP Properties of the Newly Designed PCB Molecules

Density functional theory was employed to calculate the quantum chemical descriptors (total energy, energy gap, C-Cl bond dissociation enthalpies, frequency, Gibbs free energy) at the B3LYP/6-31G* level based on Gaussian 09 software [28]. The changes in functional parameters before and after PCB-52 modification were calculated to verify whether the novel PCB molecules could be generated spontaneously.

The established QSAR models in the literature were applied to predict the other three POP characteristics (environmental persistence [26], bioconcentration [29] and biotoxicity [30]) of novel PCB-52 molecules and to verify the reliability of the 3D-QSA^{2}R model for designing environmentally friendly PCB molecular methods.

Results and Discussion

Evaluation and Analysis of the 3D-QSA^{2}R Model Based on the *Z* Values of PCBs

Since it is generally accepted that the ratio of the dependent variable number should at least satisfy 3 times the number of independent variables [31, 32], the training set and test set were divided according to the ratio of 4:1 in order to construct the 3D-QSA^{2}R model. The parameters of the CoMFA model were analysed and assessed to ensure the stability of the model. The results showed that the cross-validation coefficient (q^2) and the optimum number of components (n) were 0.842 (q^2>0.5) and 10, respectively, possibly indicating a good internal predictive ability of the CoMFA model. The non-cross-validation (R^2) and the standard error of estimated (SEE) were 0.999 (R^2>0.9) and 0.007 for the CoMFA model, respectively, where two parameters conform to the requirements for model stability. These results showed that the model had good fitting and predictive abilities (Table 2).

The external validation parameters r^2_{pred} and SEP were calculated to be 0.902 (>0.6) and 0.062, respectively, indicating that the CoMFA model has a high external prediction ability (Table 2). Linear fitting was performed on the *Z* value and its predicted value of the test set and training set to further verify the accuracy of the model prediction. The results showed that *Z* values predicted by the CoMFA model had a strong linear dependence (R^2 of 0.999, slope of 0.9991), which could be observed from the scatter plot of the *Z* values (Fig. 1).

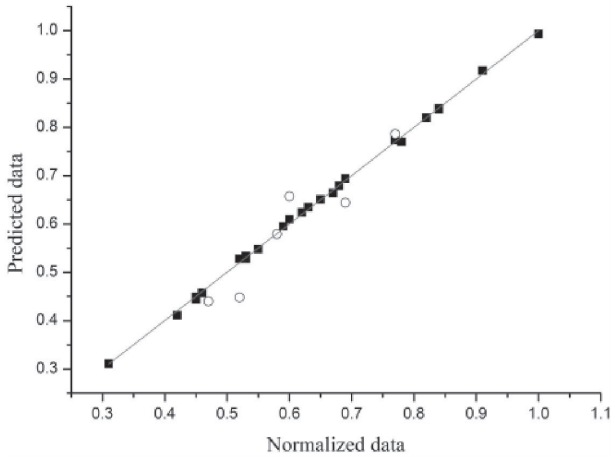

Fig. 1. Scatter plot of normalized vs. predicted Z values using the CoMFA model.

The *Z* values of 30 polyhalogenated biphenyls were predicted by the CoMFA model (Table 3). The comparison error between the normalized values of 30 molecules and their predicted values was less than 10%, which is acceptable for small base values [17].

Molecular Design of the Novel PCB-52 with Low Migration Ability

PCB-52 was used as an example to comprehensively analyze the steric field and the electrostatic field of a molecule in the contour maps of the CoMFA model (Fig. 2). In the steric field contour map (A), the yellow regions were mapped near the 2'-, 3-, 3'-, 4'-, 5'-, and 6-positions of biphenyls and its skeleton, indicating that reducing the volume of the substituents at these sites could improve the *Z* values of PCB molecules. In the electrostatic field contour map (B), the blue regions were mapped near the 2'- and 5-positions, and the red regions were mapped close to the 6'-position, indicating that the substituents replaced with electropositive groups at the 2'- and 5-positions and replaced with electronegative groups at the 6'-position could improve the *Z* values of PCB molecules (Fig. 2). A comprehensive comparison of the two kinds of force fields reveals that the 2'-position is affected by both the steric and electrostatic fields, that is, replacing the chlorine substituent with a lower volume of substituents and positive groups could improve the *Z* values for PCB-52 molecule modification.

Table 2. Evaluation parameters of the CoMFA model.

Model	q^2	n	SEE	R^2	F	r^2_{pred}	SEP
CoMFA	0.842	10	0.007	0.999	1322.458	0.902	0.062

Table 3. Comparison of changes in *Z* values after the CoMFA model simulation.

Molecule	Position of chlorine/bromine substitution	*Z*	CoMFA	
			Pred.	Relative error (%)
PCB-52	2,2',5,5'-Tetrachlorobiphenyl	0.46	0.46	0.00
PCB-101	2,2',4,5,5'-Pentachlorobiphenyl	0.53	0.53	0.00
PCB-138	2,2',3,4,4',5'-Hexachlorobiphenyl	0.62	0.62	0.00
PCB-153[a]	2,2',4,4',5,5'-Hexachlorobiphenyl	0.60	0.65	8.33
PCB-180	2,2',3,4,4',5,5'-Heptachlorobiphenyl	0.68	0.68	0.00
PBB-15	4,4'-Dibromobiphenyl	0.45	0.44	-2.22
PBB-26[a]	2,3',5-Tribromobiphenyl	0.52	0.47	-9.62
PBB-31	2,4',5-Tribromobiphenyl	0.53	0.53	0.00
PBB-49	2,2',4,5'-Tetrabromobiphenyl	0.60	0.61	1.67
PBB-103	2,2',4,5',6-Pentabromobiphenyl	0.67	0.66	-1.49
PBB-153	2,2',4,4',5,5'-Hexabromobiphenyl	0.84	0.84	0.00
PBDE-1	2-Bromodiphenyl ether	0.31	0.31	0.00
PBDE-10	2,6-Dibromodiphenyl ether	0.42	0.41	-2.38
PBDE-13[a]	3,4'-Dibromodiphenyl ether	0.47	0.44	-6.38
PBDE-15	4,4'-Dibromodiphenyl ether	0.48	0.45	-6.25
PBDE-30	2,4,6-Tribromobiphenyl ether	0.52	0.53	1.92
PBDE-32	2,4',6-Tribromobiphenyl ether	0.55	0.55	0.00
PBDE-35[a]	3,3',4-Tribromobiphenyl ether	0.58	0.58	0.00
PBDE-37	3,4,4'-Tribromobiphenyl ether	0.59	0.60	1.69
PBDE-47	2,2',4,4'-Tetrabromobiphenyl ether	0.65	0.65	0.00
PBDE-66	2,3',4,4'-Tetrabromobiphenyl ether	0.69	0.69	0.00
PBDE-75	2,4,4',6-Tetrabromobiphenyl ether	0.63	0.64	1.59
PBDE-77[a]	3,3',4,4'-Tetrabromobiphenyl ether	0.69	0.64	-7.25
PBDE-99	2,2',4,4',5-Pentabromobiphenyl ether	0.78	0.77	-1.28
PBDE-116	2,3,4,5,6-Pentabromobiphenyl ether	0.77	0.77	0.00
PBDE-119[a]	2,3',4,4',6-Pentabromobiphenyl ether	0.77	0.79	2.60
PBDE-153	2,2',4,4',5,5'-Hexabromobiphenyl ether	0.84	0.84	0.00
PBDE-155	2,2',4,4',6,6'-Hexabromobiphenyl ether	0.82	0.82	0.00
PBDE-166	2,3,4,4',5,6-Hexabromobiphenyl ether	0.91	0.92	1.10
PBDE-181	2,2',3,4,4',5,6-Heptabromobiphenyl ether	1.00	0.99	-1.00

a. (Test set)

Two new PCB-52 molecules with *Z* values that increased by 30.44% and 41.30%, respectively, were designed by molecular modification of the PCB-52 molecules with maximum migration ability in the training set (Table 4). The EPI database was used to predict the $\log K_{OA}$ and $\log P_L$ values of the two new molecules. The results showed that the $\log K_{OA}$ and $\log P_L$ parameters before and after PCB-52 modification showed basically the same trend as the *Z* values, and when the $\log K_{OA}$ of the two new molecules was reduced to its original value of K_{OA}, the K_{OA} values of 2'-methoxy-PCB-52 and 2'-vinyl-PCB-52 were significantly increased by 151.19% and 91.43%, respectively. The values of the $\log K_{OA}$ parameter of the novel PCB-52 molecules were slightly increased, which may be related to the use of the no-weight redistribution coefficient in this paper. Therefore, further research should consider improving the weight distribution coefficient of $\log K_{OA}$.

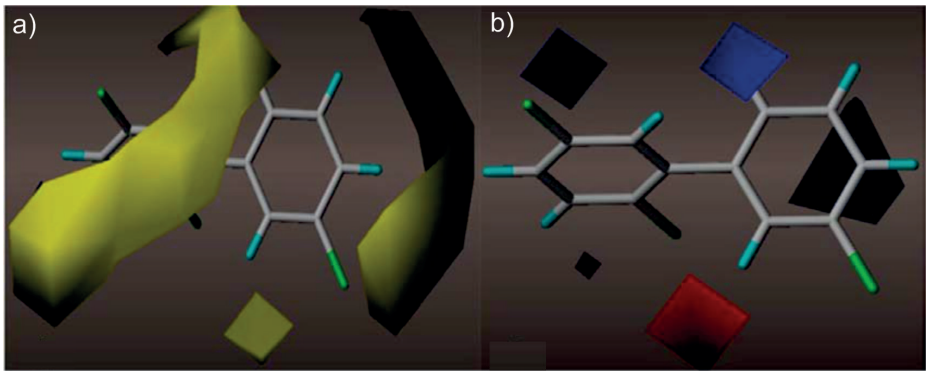

Fig. 2. Contour maps of the CoMFA model: steric fields a) and electrostatic fields b).

Table 4. Variations in the Z value, -logP_L and logK_{OA} before and after PCB-52 modification.

Type	Molecule	Z Value		-logP_L		P_L	log$_{KO}$A		K_{OA}
		Prediction	Change rate (%)	Prediction	Change Rate (%)	Change Rate (%)	Prediction	Change rate (%)	Change rate (%)
Target molecule	PCB-52	0.46	-	1.73	-	-	8.76	-	-
New molecule	2'-methoxy-PCB-52	0.60	30.44	3.10[a]	79.19	95.73	9.16[a]	4.57	151.19
	2'-vinyl-PCB-52	0.65	41.30	3.02[a]	74.57	94.87	9.04[a]	3.20	91.43

a. -logP_L and logK_{OA} parameters predicted by the EPI database as follows: (https://www.epa.gov/tsca-screening-tools/epi-suitetm-estimation-program-interface).

An analysis of the influence of the weight distribution coefficient on the comprehensive values (Z) to avoid the problem of the Z value not accurately expressing the multi-activity attribute of pollutants in the process of molecular design is needed.

Evaluation of the Functional Parameters and POP Properties of the Novel PCB-52 Molecules

The quantum chemical descriptors (total energy, energy gap, C-Cl bond dissociation enthalpies, frequency, Gibbs free energy) were calculated at the B3LYP/6-31G* level. The results showed that the total energy before and after PCB-52 modification decreased significantly, and the energy gap of novel PCB-52 molecules remained basically consistent with the PCB-52 target molecule, indicating that the insulation of the novel PCB-52 molecules remained unchanged with enhanced stability [26]. Since the PCB-52 molecule involved multiple chlorine substituents, the minimum C-Cl bond dissociation enthalpy was selected as the parameter for evaluating the flame-retardant efficiency (functional characteristics) [33]. The calculation shows that the C-Cl bond dissociation enthalpy remains unchanged after PCB-52 molecule modification, indicating that the flame retardancy of the new PCB-52 molecules was not affected (Table 5). With target molecule PCB-52 and new substituents as reactants and the novel PCB-52 molecules as products, the thermodynamic parameters such as the Gibbs free energy (ΔG) of reactants and products were calculated to determine the possible reaction path [34]. The above calculations showed that the ΔG of the two new PCB-52 molecules in the substitution reaction path was basically unchanged, indicating that the substitution reactions occurred spontaneously; that is, two new PCB-52 molecules could be generated.

Table 5. Quantum chemistry descriptors for the new PCB-52 molecules.

Type	Molecule	Total energy (a.u.)	Energy gap (a.u.)	Frequency (cm^{-1})	C-Cl bond dissociation enthalpy (kcal/mal)	ΔG (a.u.)
Target molecule	PCB-52	-2301.68	0.21	7.66	123.43	
New molecule	2'-methoxy-PCB-52	-1956.61	0.19	23.6	125.06	-0.65
	2'-vinyl-PCB-52	-1919.48	0.18	27.01	123.68	-0.02

Table 6. Prediction of environmental persistence, bioconcentration and toxicity of the newly designed PCB-52 molecules.

Type	Molecule	log$t_{1/2}$	Change rate (%)	logK_{OW}	Change rate (%)	pEC50	Change rate (%)
Target molecule	PCB-52	0.89	-	7.67	-	3.43	-
New molecule	2'-methoxy-PCB-52	0.86	-3.37	5.61	-26.86	3.47	1.17
	2'-vinyl-PCB-52	0.81	-8.99	5.62	-26.73	3.31	-3.50

To evaluate the POP characteristics of novel PCB molecules, 3D-QSAR models constructed in literature were applied to predict their environmental persistence (log$t_{1/2}$) [26], bioconcentration (logK_{OW}) [29] and toxicity (pEC_{50}) [30], respectively. As shown in Table 6, the predicted POP characteristic parameters of the two new PCB-52 molecules showed a downward trend, and the toxicity parameters of the 2'-methoxy-PCB-52 molecule increased by only 1.17%, which is a change range of less than 5%, indicating that there was no significant change in the toxicity before and after PCB-52 modification [17]. In summary, by considering the double activities of pollutants and their structural relations, the 3D-QSA²R model constructed in this paper was used to design and screen two new environmentally friendly PCB-52 molecules with a low migration ability, thus enabling environmental risk control from the source of chemical substances.

Conclusions

In this paper, the 3D-QSA²R model (employing the comprehensive characterization of the K_{OA} and P_L parameters) was established by a log-normalized method and applied to the modification design to lower the migration ability of environmentally friendly PCB molecules. The traditional 3D-QSAR model proves that the proposed 3D-QSA²R method can theoretically achieve molecular modification while considering the multi-activities of pollutants at the same time. In future work, research on the 3D-QSA²R model should focus on the weight redistribution problem between multi-activities to accurately improve the multi-activities attribute of pollutants in the process of molecular design.

Acknowledgements

We thank American Journal Experts (AJE) for English language editing. This work was supported by the Key Projects in the National Science and Technology Pillar Program in the 11th Five-Year Plan Period (No. 2008BAC43B01).

Conflicts of Interest

The authors declare no conflict of interest.

References

1. SCHERINGER M. Long-range transport of organic chemicals in the environment. Environmental Toxicology and Chemistry, **28** (4), 677, **2009**.
2. MACKAY D., WANIA F. Transport of contaminants to the Arctic: Partitioning, processes and models. Science of the Total Environment, **160**, 25, **1995**.
3. RAPPAPORT S.M., SMITH M.T. Environment and disease risks. Science, **330** (6003), 460, **2010**.
4. LINTHORST J.A. An overview: origins and development of green chemistry. Foundations of Chemistry, **12** (1), 55, **2010**.
5. TERZAGHI E., ZANARDINI E., MOROSINI C., RASPA G., BORIN S., MAPELLI F., VERGANI L., GUARDO A.D. Rhizoremediation half-lives of PCBs: Role of congener composition, organic carbon forms, bioavailability, microbial activity, plant species and soil conditions, on the prediction of fate and persistence in soil. Science of The Total Environment, **612**, 544, **2018**.
6. ADAMS M.C., BAKER J.E., KJELLERUP B.V. Toxicological effects of polychlorinated biphenyls (PCBs) on freshwater turtles in the United States. Chemosphere, **154**, 148, **2016**.
7. RANJBAR J.A., RIYAHI B.A., ALIABADIAN M., LAETITIA H., SHADMEHRI T.A., YAP C.K. First report of bioaccumulation and bioconcentration of aliphatic hydrocarbons (AHs) and persistent organic pollutants (PAHs, PCBs and PCNs) and their effects on alcyonacea and scleractinian corals and their endosymbiotic algae from the Persian Gulf, Iran: Inter and intra-species differences. Science of The Total Environment, **627**, 141, **2018**.
8. GIOIA R., NIZZETTO L., LOHMANN R., Dachs J., TEMME C., JONES K.C. Polychlorinated biphenyls (PCBs) in air and seawater of the Atlantic Ocean: sources, trends and processes. Environmental Science and Technology, **42** (5), 1416, **2016**.
9. ODABASI M., CETIN E., SOFUOGLU A. Determination of octanol-air partition coefficients and supercooled liquid vapor pressures of PAHs as a function of temperature: Application to gas-particle partitioning in an urban atmosphere. Atmospheric Environment, **40** (34), 6615, **2006**.
10. LOHMANN R., LAMMEL G. Adsorptive and absorptive contributions to the gas-particle partitioning of polycyclic aromatic hydrocarbons: state of knowledge and recommended parametrization for modeling. Environmental Science and Technology, **38** (14), 3793, **2004**.
11. XIAO H., WANIA F. Is vapor pressure or the octanol–air partition coefficient a better descriptor of the partitioning between gas phase and organic matter. Atmospheric Environment, **37** (20), 2867, **2003**.

12. CHEN J.W., YANG P., CHEN S., QUAN X., YUAN X., SCHRAMM K.W., KETTRUP A. Quantitative structure-property relationships for vapor pressures of polybrominated diphenyl ethers. SAR and QSAR in Environmental Research, **14** (2), 97, **2003**.
13. YUAN Y., SUN Y., WANG D., LIU R., GU S., LIANG G., XU J. Quantitative structure-property relationship study of liquid vapor pressures for polychlorinated diphenyl ethers. Fluid Phase Equilibria, **391**, 31, **2015**.
14. KATRIZKY A.R., SLAVOV S.H., DOBCHEV D.A., KARELSON M. Rapid QSPR model development technique for prediction of vapor pressure of organic compounds. Computers and Chemical Engineering, **31** (9), 1123, **2007**.
15. FU Z., CHEN J, LI X., WANG Y. Comparison of prediction methods for octanol-air partition coefficients of diverse organic compounds. Chemosphere, **148** (4), 118, **2016**.
16. YUAN J., YU S., ZHANG T., YUAN X., CAO Y., YU X., YANG X., YAO W. QSPR models for predicting generator-column-derived octanol/water and octanol/air partition coefficients of polychlorinated biphenyls. Ecotoxicology and Environmental Safety, **128**, 171, **2016**.
17. CHEN Y., CAI X., JIANG L., LI Y. Prediction of octanol-air partition coefficients for polychlorinated biphenyls (PCBs) using 3D-QSAR models. Ecotoxicology and Environmental Safety, **124**, 202, **2016**.
18. REN, Z.X., WANG Y.W., XU, H.H., LI Y.F., Han S. Fuzzy comprehensive evaluation assistant 3D-QSAR of environmentally friendly FQs to reduce ADRs. International Journal of Environmental Research and Public Health, **16**, 3161, **2019**.
19. JAIN A., NANDAKUMAR K., ROSS A. Score normalization in multimodal biometric systems. Pattern Recognition, **38** (12), 2270, **2005**.
20. COLAN M.D., STEVEN D. The why and how of Z scores. Journal of the American Society of Echocardiography, **26** (1), 38, **2013**.
21. HAMPEL F.R., RONCHETTI E., ROUSSEEUW P., STAHEL W.A. Robust statistics: the approach based on influence functions. Technometrics, **29** (2), 240, **1987**.
22. LIN Q.X., SHI S.Z., LI S.S., LI L., LI J., YU Z.L. Application of well log normalization in coalfield seismic inversion. Journal of Coal Science and Engineering (China), **19** (2), 167, **2013**.
23. SEPPÄ K., HAKULINEN T., LÄÄRÄ E., PITKÄNIEMI J. Comparing net survival estimators of cancer patients. Statistics in Medicine, **35** (11), 1866, **2016**.
24. VALKÓ P.P., VAJDA S. Inversion of noise-free laplace transforms: towards a standardized set of test problems. Inverse Problems in Engineering, **10** (5), 467, **2002**.
25. ZHAO H.X. Basic research on chemical characterization and oxidation degradation of brominated flame retardants. Chinese Academy of Science (Dalian Institute of Chemical Physics), **2006** [In Chinese].
26. XU Z., CHEN Y., QIU Y., GU W., LI Y. Prediction of stability for polychlorinated biphenyls in transformer insulation oil through three-dimensional quantitative structure-activity relationship pharmacophore model and full factor experimental design. Chemical Research in Chinese Universities, **32** (3), 348, **2016**.
27. HAO C.Z., XIA S.W., WANG H., XUE J., YU L.M. Using 3D-QSAR and molecular docking insight into inhibitors binding with complex-associated kinases CDK8. Journal of Molecular Structure, **1173**, 498, **2018**.
28. QU R.J., LIU J.Q., LI C.G., WANG L.S., WANG Z.Y., WU J.C. Experimental and theoretical insights into the photochemical decomposition of environmentally persistent perfluorocarboxylic acids. Water Research, **104**, 34, **2016**.
29. YANG J., GU W., LI Y. Biological Enrichment prediction of polychlorinated biphenyls and novel molecular design based on 3D-QSAR/HQSAR associated with molecule docking. Bioscience Reports, **39** (5), **2018**.
30. LI F., LI X., LIU X., ZHANG L., YOU L., ZHAO J., WU, H. Docking and 3D-QSAR studies on the receptor binding affinities of polychlorinated biphenyls (PCBs), dibenzo-p-dioxins (PCDDs) and dibenzofurans (PCDFs). Environmental Toxicology and Pharmacology, **32** (3), 478, **2011**.
31. QIU Y.L., LI Y. A theoretical method for the high-sensitivity fluorescence detection of PAEs through double-substitution modification. Environmental Science and Pollution Research, **25**, 34684, **2018**.
32. TOPLISS J.G., EDWARDS R.P. Chance factors in studies of quantitative structure-activity relationships. Journal of Medicinal Chemistry, **22**, 1238, **1979**.
33. CAO D., YAN C., ZHOU P., ZENG H.Y., LI C.J. Hydrogen bonding promoted simple and clean photo-induced reduction of C-X bond with isopropanol. Chemical Communications, **55** (6), 767, **2018**.
34. DOLFING J., NOVAK I. The Gibbs free energy of formation of halogenated benzenes, benzoates and phenols and their potential role as electron acceptors in anaerobic environments. Biodegradation, **26** (1), 15, **2015**.